

Reinterpreting the Cu–Pd phase diagram based on new ground-state predictions

This content has been downloaded from IOPscience. Please scroll down to see the full text.

2007 J. Phys.: Condens. Matter 19 032201

(<http://iopscience.iop.org/0953-8984/19/3/032201>)

View [the table of contents for this issue](#), or go to the [journal homepage](#) for more

Download details:

IP Address: 198.11.29.40

This content was downloaded on 04/03/2017 at 16:41

Please note that [terms and conditions apply](#).

You may also be interested in:

[Bulk and surface ordering phenomena in binary metal alloys](#)

Stefan Müller

[Finding the lowest-energy crystal structure starting from randomly selected lattice vectors and atomic positions: first-principles evolutionary study of the Au–Pd, Cd–Pt, Al–Sc, Cu–Pd, Pd–Ti, and Ir–N binary systems](#)

Giancarlo Trimarchi and Alex Zunger

[Short-range-order types in binary alloys: a reflection of coherent phase stability](#)

C Wolverton, V Ozolins and Alex Zunger

[Predicting the segregation profile of the Pt₂₅Rh₇₅\(100\) surface from first-principles](#)

P Welker, O Wieckhorst, T C Kerscher et al.

[Configurational thermodynamics of alloys from first principles: effective cluster interactions](#)

A V Ruban and I A Abrikosov

[Thermodynamic theory of epitaxial alloys: first-principles mixed-basis cluster expansion of \(In, Ga\)N alloy film](#)

Jefferson Zhe Liu and Alex Zunger

FAST TRACK COMMUNICATION

Reinterpreting the Cu–Pd phase diagram based on new ground-state predictions

S Bärthlein¹, G L W Hart², A Zunger³ and S Müller¹¹ University Erlangen-Nürnberg, Lehrstuhl für Festkörperphysik, Staudtstraße 7, D-91058 Erlangen, Germany² Department of Physics and Astronomy, Brigham Young University, Provo, UT 84602, USA³ National Renewable Energy Laboratory, Golden, CO 80401, USAE-mail: stefan.mueller@physik.uni-erlangen.de

Received 9 November 2006, in final form 18 December 2006

Published 5 January 2007

Online at stacks.iop.org/JPhysCM/19/032201**Abstract**

Our notions of the phase stability of compounds rest to a large extent on the experimentally assessed phase diagrams. Long ago, it was assumed that in the Cu–Pd system for $x_{\text{Pd}} \leq 25\%$ there are at least two phases at high temperature ($L1_2$ and a $L1_2$ -based superstructure), which evolve into a single $L1_2$ -ordered phase at low temperature. By constructing a first-principles Hamiltonian, we predict a yet undiscovered Cu_7Pd ground state at $x_{\text{Pd}} = 12.5\%$ (referred to as S1 below) and an $L1_2$ -like Cu_9Pd_3 superstructure at 25% (referred to as S2). We find that in the low-temperature regime, a single $L1_2$ phase cannot be stable, even with the addition of anti-sites. Instead we find that an S2-phase with S1-like ordering tendency will form. Previous short-range order diffraction data are quantitatively consistent with these new predictions.

(Some figures in this article are in colour only in the electronic version)

At low temperatures, binary A_{1-x}B_x alloys either phase-separate into their constituents or order crystallographically on a given lattice. In the latter case, one expects a set of ordered compounds (ground states) A_pB_q at $T = 0$ K occurring at discrete stoichiometric compositions $X_p = p/(p + q)$, whereas for samples with concentrations between adjacent X_p values there will be mixtures of the ‘neighbouring’ ground states. A central problem in the field of alloy phase stability is to structurally characterize single phases of compounds and distinguish them from mixtures in the phase diagram. This is often done by diffraction experiments (at temperatures below the order–disorder transitions) or via diffuse scattering short-range order (SRO) measurements (at temperatures above the order–disorder transition).

As critical as this distinction is to our understanding of phase stability, it is not always obvious. The dashed box in figure 1 traces the previously assessed phase diagram [1] of Cu–Pd between 10% and 30% Pd, showing two phases assigned to the composition Cu_3Pd :

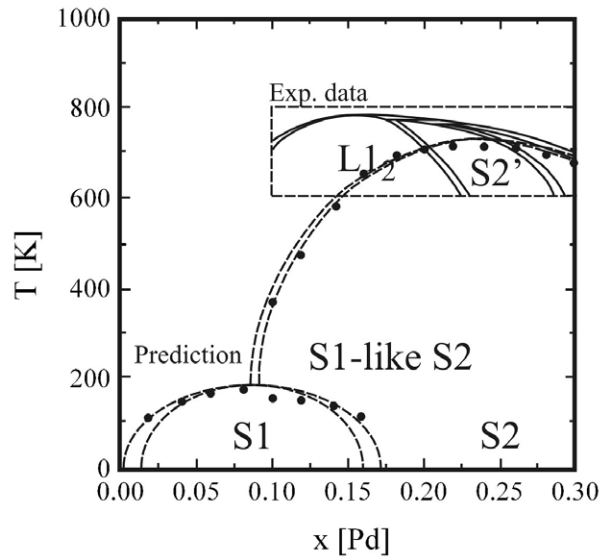


Figure 1. Phase diagram of Cu–Pd in the Cu-rich region. For $T > 600$ K, the phase boundaries proposed in [1] ('Exp. data') are plotted. The low-temperature phase S1 is not accessible experimentally. The structures S1 and S2 are shown in figure 2. Around $x_{\text{Pd}} \approx 20\%$, we predict an S1-like S2, not the previously proposed $L1_2$ ordered phase. The dashed lines display the *coherent* phase boundaries obtained via a Monte Carlo simulation of our cluster expansion, including proposed two-phase regions.

one denoted $L1_2$ and another denoted $S2'$, being a generic term for a whole class of long-period superstructures (LPS) based on an $L1_2$ motif. Two representative structures in this class ($S2$ and $L1_2$) are depicted in figure 2. This assignment was based on high resolution electron microscopy (HREM) studies by Broddin *et al* [2, 3] and earlier studies collected in [1]. Saha [4] and Oshima *et al* [5, 6] measured the diffuse intensity of x-ray diffraction experiments of quenched samples, which was used to assign the $L1_2$ /LPS structure on the basis of the peaks occurring at the composition of $x_{\text{Pd}} = 29.8\%$ at $T = 773$ K: as the fundamental wavevector of an $L1_2$ -based superstructure with period M is given by $\mathbf{k} = (1, 1/2M, 0)$, $M = 3$ denotes the LPS 3 structure as the underlying ground state. The kinetics of LPS formation in this region of the phase diagram is qualitatively understood [7].

Despite such detailed measurements, a number of puzzles remain: (i) despite $L1_2$ being nominally a 3:1 stoichiometry, the observed phase is centred around 15% Pd, not 25% (inset to figure 1). Although many binary alloys exhibit such a behaviour, a deviation of 10% is rather large. We will show later that the ground state is not a 3:1 $L1_2$ structure but rather a 7:1 Cu_7Pd structure. (ii) At ≈ 650 K there are two ordered phases, but due to the difficulty in assessing experimentally the low-temperature thermodynamic configurations on account of kinetic barriers, one does not know which of these phases, if any, is a ground state. In [8–11], $L1_2$ was found to be less stable than $S2$ -like structures; however, the side-by-side existence of these two structures at higher temperatures could not be explained.

In order to understand these puzzles in this classic alloy system we have carried out a first-principles cluster expansion study. The total energies of $\mathcal{O}(50)$ different ordered configurations, calculated via LDA, are mapped onto a generalized Ising-like Hamiltonian where the many-body interaction types (MBITs) are selected via a genetic algorithm [12, 13]. Once established, this cluster expansion is searched, identifying all possible $T = 0$ K ground-state structures,

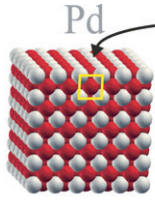
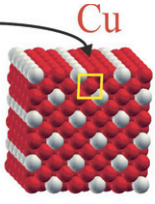
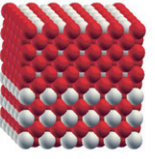
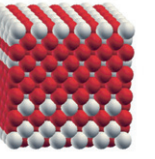
Name	L1 ₂	S1	S2 (LPS3)	S3
Crystal structure				
	Cu ₃ Pd	Cu ₇ Pd	Cu ₉ Pd ₃	Cu ₈ Pd ₄
x _{Pd}	1/4	1/8	1/4	1/3
Lattice vectors	$\begin{pmatrix} 1 & 0 & 0 \\ 0 & 1 & 0 \\ 0 & 0 & 1 \end{pmatrix}$	$\begin{pmatrix} 1 & 0 & 0 \\ 0 & 1 & 1 \\ 0 & \bar{1} & 1 \end{pmatrix}$	$\begin{pmatrix} 1 & 0 & 0 \\ 0 & 1 & 0 \\ \frac{1}{2} & \frac{1}{2} & 3 \end{pmatrix}$	$\begin{pmatrix} 1 & 0 & 0 \\ 0 & 1 & 0 \\ \frac{1}{2} & \frac{1}{2} & 3 \end{pmatrix}$

Figure 2. The ground-state structures S1, S2 and S3, all related to L1₂ directly or to an L1₂ superstructure incorporating antiphase boundaries. These structures belong to the space group $P\frac{4}{m}mm$ (i.e. D_{4h}^1 in Schoenflies nomenclature).

and, via finite temperature Monte Carlo studies using the same Hamiltonian, the SRO and the phase diagram at low temperatures are calculated.

We find that (i) the L1₂ structure is not a ground state. Instead, at the Cu₃Pd composition the ground state is S2 (shown in figure 2). (ii) There is another, previously unrecognized, ground state Cu₇Pd (S1) at $x_{Pd} = 12.5\%$ (see also figure 2). (iii) The central feature of the experimental phase diagram in the composition range $x_{Pd} = 5\%–30\%$ does not correspond to a single L1₂ phase, but rather to an S2 phase containing S1-like defects. (iv) The calculated SRO agrees well with experimental observations, demonstrating the validity of our model. (v) A comparison between the formation enthalpy for the S1-like S2 and an L1₂ phase containing antisites predicts the formation of the former, ruling out the latter. Our study exemplifies how even well-established phase phenomena in classic alloy systems can be challenged via first-principles statistical mechanics and calls for further experimental examination of this prototypical system.

Method: Our cluster expansion method is based on the mixed basis approach of Zunger and co-workers [14, 15, 10, 16]. The formation enthalpies ΔH_f are obtained from fully relaxed total energy structure calculations. These energies are mapped onto an Ising-like Hamiltonian

$$\Delta H_{CE}(\sigma) = \sum_{\mathbf{k}} J_{\text{pair}}(\mathbf{k}) |S(\mathbf{k}, \sigma)|^2 + \sum_f^{\text{MBITs}} D_f J_f \bar{\Pi}_f(\sigma) + \frac{1}{4x-1} \sum_{\mathbf{k}} J_{CS}(x, \hat{\mathbf{k}}) |S(\mathbf{k}, \sigma)|^2. \quad (1)$$

Herein, the lattice-averaged spin product $\bar{\Pi}_f(\sigma)$ of a figure f for a given configuration σ times its degeneracy D_f is weighted by the effective energy J_f of the many-body interaction types (MBITs). In contrast, both pair interactions $J_{\text{pair}}(\mathbf{k})$ and ‘coherency–strain interactions’ $J_{CS}(x, \hat{\mathbf{k}})$ are handled in \mathbf{k} -space [15]. The latter comprise the equilibrium strain energy $E_{CS}(x, \mathbf{k})$ by which we are able to treat the long-range interactions properly.

The MBITs are determined by requiring equation (1) to reproduce a set of input LDA formation enthalpies, $\{\Delta H_{LDA}(\sigma)\}$, and to accurately predict formation enthalpies for structures outside this set. To do so, we use two sets of iterations (loops) [17]. In the internal

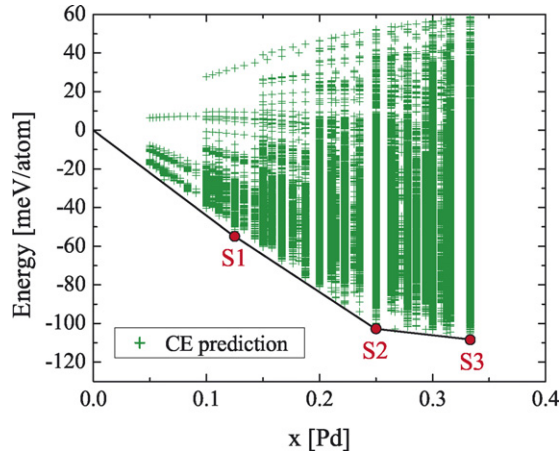


Figure 3. Ground-state diagram in the Cu-rich regime. Each triangle represents the predicted energy for one specific crystal structure. The solid line is the convex hull of all $\mathcal{O}(10^6)$ energies. The ground-state structures are depicted in figure 2. $L1_2$ is not a ground state, but rather the $L1_2$ -related superstructure S2 (LPS 3).

loop we use a genetic algorithm to select the MBITs that not only best fit the energies of the input LDA set but also predict accurately the energies of structures that are not yet included in the input set. In the outer loop we iteratively augment the set of input structures used in the fit, adding to it configurations σ identified as ground states in prior outer loop iteration. Once the CE is established, it is used to exhaustively search the energies of all $\mathcal{O}(2^{20})$ structures (figure 3), to calculate the phase diagram (figure 1) and the SRO (figure 4).

Ground-state structures: Figure 3 shows the energies of $\approx 2^{20}$ ordered configurations and indicates the breaking points of the convex hull, i.e. the ground-state structures. Figure 2 gives the structural description of the ground states. We find (a) the Cu_7Pd (S1) structure at $x_{\text{Pd}} = 12.5\%$, (b) the Cu_3Pd (S2 or LPS 3) structure at 25% and (c) the Cu_8Pd_4 (S3) structure at $x_{\text{Pd}} = 33\%$. We find that at $x_{\text{Pd}} = 25\%$ and $T = 0$ K S2 is considerably stabilized over $L1_2$ as the ground state.

Finding (b) is in agreement with [8–11]; S2 is predicted as a ground state at $x = 1/4$, lower in energy than $L1_2$: $\Delta H_f(\text{S2}) = -102.6$ meV/atom, $\Delta H_f(\text{L1}_2) = -99.8$ meV/atom. At 12.5% Lu *et al* [18] predicted the D1 structure, which, though not identical to S1, is also similar to $L1_2$. The S1 ground state is related to the $L1_2$ structure by a simple exchange of Cu and Pd rows along [100] as shown in figure 2. Previous studies (e.g. [2, 19, 20]) that obtained $L1_2$ as the ground state at $\approx 18\%$ referred to the ANNNI Ising model, or performed an electronic mean field approach [8]. However, negligence of S1 in the first-principles input [11] will favour interactions that are ‘blind’ for S1.

S1-like S2 region: Given that we predict at an S1 phase $T = 0$ K at 12.5% Pd and an S2 phase at 25% Pd, it is interesting to characterize the phase(s) at intermediate concentrations. In order to examine the energies $E_{\text{CE}}(\sigma)$ of structures with cells bigger than 20 atoms (figure 3), we constructed large $24 \times 24 \times 24$ cells and sampled their energies via Monte Carlo (vibrational entropy was not taken into account). Due to the variety of incommensurate superstructures with non-coherent phase boundaries, we have to restrict our study to low temperatures⁴—a more thorough thermodynamic study may not be feasible with Monte Carlo. Nevertheless, the

⁴ Incoherencies, originating from smoothed APB profiles and wetting around the phase transition cannot be accounted for by our MC simulation, which is restricted to the fcc lattice.

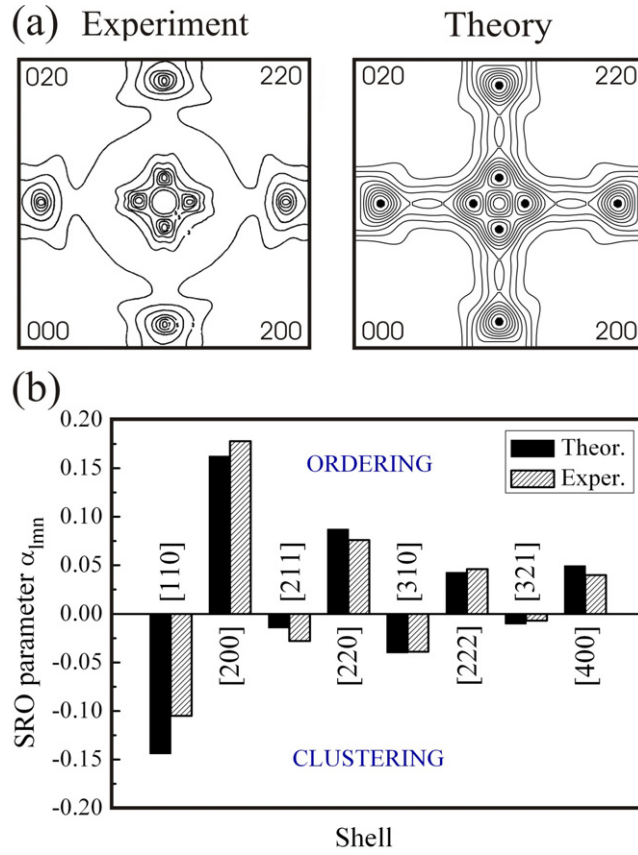


Figure 4. (a) Experimental [5] versus theoretical short-range order for $\text{Cu}_{0.702}\text{Pd}_{0.298}$ at $T = 773$ K in reciprocal space. The SRO exhibits peaks of the fundamental wavevector $\mathbf{k} = (1, 1/2M, 0)$ at $M = 3$, in excellent agreement with the superstructure period of S2. (b) Real space SRO for neighbouring pairs separated by $[lmn]$.

critical temperature $T_c \approx 800$ K for the phase transition from A1 to S2 is in good agreement with experiment ($T_c^{\text{Exp}} \approx 780$ K). Simulated annealing in the intermediate region provides indication of a transition from the disordered high temperature phase to a lower temperature S1-like S2 structure. The latter resembles LPS 3-like ordering, permeated with an S1-like pattern⁵. An investigation of the energetic hierarchies of these phases supports the hypothesis of the formation of an S1-like S2 structure.

Short-range order: In the S1-like S2 region no recent diffraction data are available in order to directly compare experimental with our calculated results, hence we examine SRO data from the region of coherency. In figure 4 we show our calculations

$$\alpha_{lmn}(x) = 1 - \frac{\langle \bar{\Pi}_{lmn} \rangle - (2x - 1)^2}{1 - (2x - 1)^2} \quad (2)$$

for 29.8% Pd, where several studies yielded comparable data. For comparison with experimental data, the so-called ‘shells’ lmn are introduced which are defined by the distance

⁵ Narrow regions of two-phase coexistence could not be captured by our MC simulation. However, such two-phase regions, even if very narrow, must exist due to Gibbs’ phase rule.

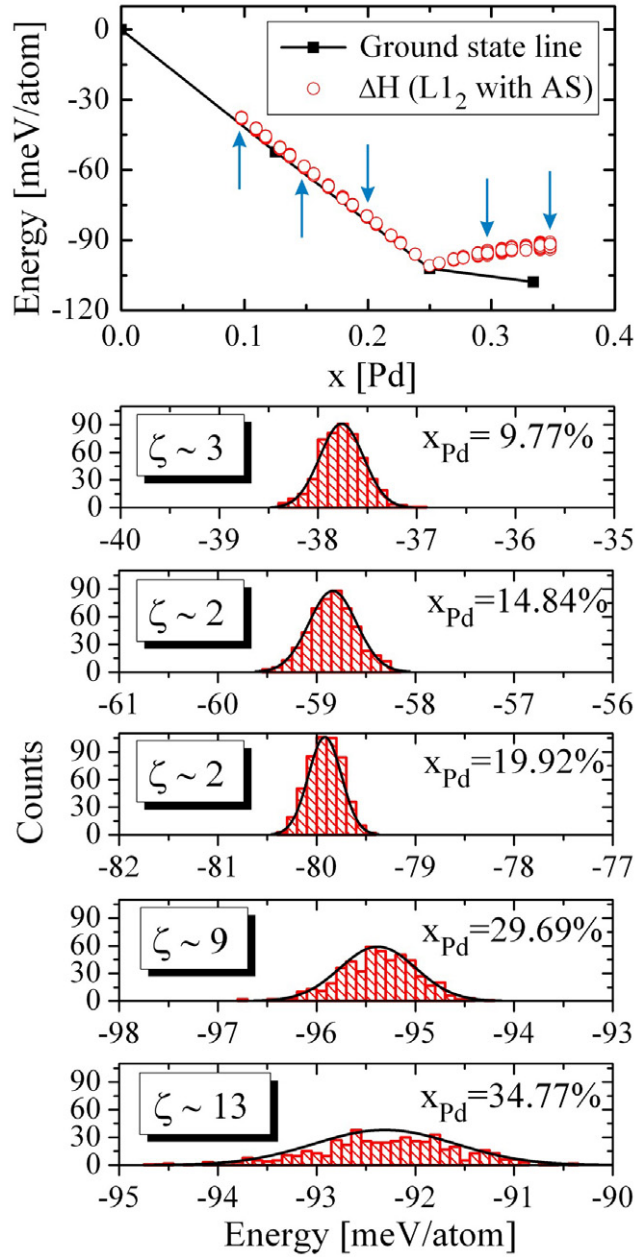


Figure 5. Predicted energies of L₁₂-based antisite structures and their distribution at various concentrations. ζ indicates the approximate distance to the ground-state line (in meV/atom) at the corresponding concentrations.

between A and B atoms in terms of half lattice parameters, $(l_{\frac{a}{2}}, m_{\frac{a}{2}}, n_{\frac{a}{2}})$, e.g. for an fcc lattice the nearest-neighbour distance would be described by the shell [110].

For $1/8 < x_{Pd} < 1/4$ the SRO connected with S1 at elevated temperatures cannot be distinguished from that of L₁₂ single phase, as S1 is a low-temperature state. Our calculations

Table 1. Comparison of LDA-calculated formation enthalpies for the crystal structures S1 (at $x_{\text{Pd}} = 1/8$), S2 = LPS 3 (at $x_{\text{Pd}} = 1/4$) and the antisite structure $\text{Cu}_{25}\text{Pd}_7$ with cluster expansion (CE) and Monte Carlo (MC) at $T = 0$ K. The latter is constructed by a $2 \times 2 \times 2$ supercell of L1_2 , including 32 atoms. One of eight Pd atoms is exchanged for a Cu atom, so the concentration goes to $7/32 = 21.875\%$. Its LDA- and CE energies are less favourable than the formation of S1-like ordered defects in the S2 region.

Structure	LDA	CE	MC
S1	-52.6	-52.3	-52.3
$\text{Cu}_{25}\text{Pd}_7$	-87.5	-87.4	—
GS line ($x = 7/32$)	-90.2	-90.0	—
S1-like S2	—	—	-89.2
S2	-102.8	-102.6	-102.6

indicated that above ≈ 400 K, even at 12.5% Pd, there is no genuine S1 peak visible any more. Concerning the HREM study of Broddin *et al* [3], which exhibits an antisite-based L1_2 -like single phase at 19.3% Pd and 613 K, we still find L1_2 -like order slightly below the phase transition, although we can already observe the S2 antiphase-based features. However, Broddin also characterizes the L1_2 domains to be separated by antiphase boundaries. Notwithstanding possible deviations, one should have in mind that these experimental indications may not represent the thermodynamic equilibrium situation.

S1-like S2 phase versus L1_2 phase with antisites: The previously mentioned question concerning the stability of an antisite-based L1_2 single phase was addressed by a systematic comparison of antisite structures with the energy of S1-like S2 structures. This is exemplified in table 1: based on a $2 \times 2 \times 2$ - L1_2 cell, one Cu atom is substituted by a Pd atom. Hence the concentration decreases from 25% to 21.875% Pd. We compared the energetic predictions for the $\text{Cu}_{25}\text{Pd}_7$ structure with the energy of a Monte Carlo cell with the same composition and found the latter to exhibit a S1-like S2, lower in energy, and hence more stable, than the antisite single phase based on L1_2 . The direct calculation with LDA verifies the accuracy and predictive power of our CE.

Subsequently, based on a $4 \times 4 \times 4$ - L1_2 , random atom flips were performed to shift the concentration to $x_{\text{Pd}} = \{10\%, \dots, 35\%\}$ in steps of 1%. For each x_{Pd} , 500 antisite configurations are predicted and compared to the ground-state line (GSL). Figure 5 gives the distribution of energies and their distance ζ (in meV/atom) from the GSL. In all cases, the ground-state line is not broken, but S1-like S2 is still more stable than a L1_2 -based phase permeated with antisites.

In summary, we find that, contrary to previous assessments, Cu–Pd (i) does not have an L1_2 ground state; (ii) instead, the Cu_3Pd S2 structure is more stable at 25% composition. (iii) A new ground state S1 is predicted at lower composition with Cu_7Pd stoichiometry, hence (iv) the features of L1_2 -like ordering observed experimentally at 17% [2] are due to a S2 phase with S1-like defects, not due to an L1_2 phase.

This work was supported by DF, Mu 1648/3, NSF DMR-0244183, and USA DOE no. DEAC36-98-GO10337.

References

- [1] Huang P, Menon S and de Fontaine D 1991 *J. Phase Equilib.* **12** 3
- [2] Broddin D, Van Tendeloo G, Van Landuyt J, Amelinckx S, Portier R, Guymont M and Loiseau A 1986 *Phil. Mag. A* **54** 395

- [3] Broddin D, Van Tendeloo G, Van Landuyt J, Amelinckx S and Loiseau A 1988 *Phil. Mag.* B **57** 31
- [4] Saha D K, Koga K and Oshima K 1992 *J. Phys.: Condens. Matter* **4** 10093
- [5] Oshima K and Watanabe D 1976 *Acta Crystallogr. A* **32** 883
- [6] Oshima K and Watanabe D 1973 *Acta Crystallogr. A* **29** 520
- [7] Wang X, Mainville J, Ludwig K, Flament X, Finel A and Caudron R 2005 *Phys. Rev. B* **72** 024215
- [8] Ceder G, de Fontaine D, Dreysse H, Nicholson D M, Stocks G M and Gyorfy B C 1990 *Acta Metall. Mater.* **38** 2299
- [9] Ruban A V, Shallcross S, Simak S I and Skriver H L 2004 *Phys. Rev. B* **70** 125115
- [10] Lu Z W, Laks D B, Wei S H and Zunger A 1994 *Phys. Rev. B* **50** 6642
- [11] Colinet C and Pasturel A 2002 *Phil. Mag.* B **82** 1067
- [12] Blum V and Zunger A 2004 *Phys. Rev. B* **70** 155108
- [13] Hart G L W, Blum V, Walorski J and Zunger A 2005 *Nat. Mater.* **4** 391
- [14] Laks D B, Ferreira L G, Froyen S and Zunger A 1992 *Phys. Rev. B* **46** 12587
- [15] Zunger A 1994 *Statics and Dynamics of Alloy Phase Transformations (NATO ASI Series)* ed E A Turchi and A Gonis (New York: Plenum) pp 361–419
- [16] Zunger A, Wang L G, Hart G L W and Sanati M 2002 *Modelling Simul. Mater. Sci. Eng.* **10** 685
- [17] Blum V, Hart G L W, Walorski M J and Zunger A 2005 *Phys. Rev. B* **72** 165113
- [18] Lu Z W, Wei S H, Zunger A, Frota-Pessoa S and Ferreira L G 1991 *Phys. Rev. B* **44** 512
- [19] Takeda S, Kulik J and de Fontaine D 1987 *Acta Metall.* **35** 2243
- [20] Takeda S, Kulik J and de Fontaine D 1988 *J. Phys. F: Met. Phys.* **18** 1387